# Viscous Interaction Theory for Slender Axisymmetric Bodies in Hypersonic Flow

H. MIRELS* AND J. W. ELLINWOOD†
*The Aerospace Corporation, El Segundo, Calif.*

**Effects of viscous interaction are investigated for hypersonic flow over slender axisymmetric bodies. The entire range of interaction, from weak to strong, is considered. Extensive numerical results are given for the self-similar flow over a $\frac{3}{4}$ power-law body. These results are correlated and used in a local similarity procedure for finding viscous interaction over arbitrary slender body shapes. Analytical expressions are derived for weak interaction on a cone and strong interaction on all slender bodies. Numerical solutions needed for the intermediate interaction regime are obtained for hypersonic flow over a cone. Results are presented for cone surface pressure, shear, heat transfer, drag, and displacement thickness in all interaction regimes. The drag data are in agreement with available experimental cone drag data. This analytical development is a unified treatment of viscous interaction effects on two-dimensional as well as axisymmetric bodies.**

## Nomenclature

$A$ = transverse curvature parameter, Appendix A
$B$ = transverse curvature parameter, Eqs. (5)
$C$, $C_w$ = $\bar{\mu}_m\bar{T}_\infty/\bar{\mu}_\infty\bar{T}_m$, $\bar{\mu}_w\bar{T}_\infty/\bar{\mu}_\infty\bar{T}_w$, respectively
$C_D$ = drag coefficient referenced to base area, $2\bar{D}/\bar{\rho}_\infty\bar{u}_\infty{}^2\bar{A}_B$
$F(\xi,\eta)$ = boundary-layer stream function, Eqs. (5)
$g(\xi,\eta)$ = $H/H_e$
$g_{wi}$ = insulated wall value of $g_w$
$H$, $\bar{H}$ = stagnation enthalpy, $H = 2\bar{H}/\bar{u}_\infty{}^2$
$h$, $\bar{h}$ = static enthalpy, $h = 2\bar{h}/\bar{u}_\infty{}^2$
$J_e$ = $\int_0^\infty (g - F_\eta{}^2)d\eta$
$\bar{L}$ = axial length of vehicle
$M_\infty$ = freestream Mach number
$m$, $m_e$ = power-law body exponents, $r_w \sim x^m$ and $r_e \sim x^{m_e}$
$Pr$ = Prandtl number
$p_e$, $\bar{p}_e$ = pressure in boundary layer, $p_e = \bar{p}_e/\alpha^2\bar{\rho}_\infty\bar{u}_\infty{}^2$
$q_w$, $\bar{q}_w$ = local heat transfer, Eqs. (8)
$R$ = $(r/r_w)^{\sigma+1}$
$Re$ = Reynolds number, $\bar{\rho}_\infty\bar{u}_\infty\bar{L}/\bar{\mu}_\infty$
$r$, $\bar{r}$ = lateral distance, $r = \bar{r}/\alpha\bar{L}$
$r_w(x)$, $\bar{r}_w(\bar{x})$ = wall ordinate
$\bar{T}$, $\bar{T}_0$ = static temperature, freestream stagnation temperature
$u$, $\bar{u}$ = axial velocity, $u = \bar{u}/\bar{u}_\infty$
$v$, $\bar{v}$ = lateral velocity, $v = \bar{v}/\alpha\bar{u}_\infty$
$x$, $\bar{x}$ = axial distance, $x = \bar{x}/\bar{L}$
$\alpha$ = characteristic body slope, $\bar{r}_w(\bar{L})/\bar{L}$
$\alpha_s$ = characteristic shock slope, $\bar{r}_s(\bar{L})/\bar{L}$
$\beta$ = pressure gradient parameter, Eqs. (5)
$\gamma$ = ratio of specific heats
$\delta$, $\delta^*$, $\bar{\delta}$ = boundary-layer thickness, displacement thickness, $\delta = \bar{\delta}/\alpha\bar{L}$
$\zeta$ = $r_e/r_s$
$\eta$ = transformed ordinate, Eqs. (3)
$\Lambda$ = interaction parameter, $(M_\infty/\alpha^2)(C/Re)^{1/2}$
$\Lambda_x$ = local value of interaction parameter $(x/r_w)^2 \times \Lambda/(x)^{1/2}$
$\mu$, $\bar{\mu}$ = viscosity, $\mu = \bar{\mu}/\bar{\mu}_\infty$
$\xi$ = transformed axial distance, Eqs. (3)
$\rho$, $\bar{\rho}$ = density, $\rho = \bar{\rho}/\bar{\rho}_\infty$
$\sigma$ = 0, 1 for two-dimensional and axisymmetric flows, respectively
$\tau_w$, $\bar{\tau}_w$ = local wall shear, Eqs. (8)

***Subscripts***

$e$ = value at outer edge of boundary layer
in = inviscid flow value
$m$ = evaluated at mean temperature
$s$ = value at shock
$w$ = value at wall
$\infty$ = value at freestream

***Superscripts***

$(^-)$ = dimensional quantity
$(')$ = $d(\ )/dx$

Received November 1, 1967; also presented as Paper 68-1 at the AIAA 6th Aerospace Sciences Meeting, New York, January 22–24, 1968; revision received June 26, 1968. This study was conducted under Air Force Contract F04695-67-C-0158. The authors are indebted to E. H. Fletcher, to H. S. Porjes and B. A. Troesch, and to V. B. Cook for machine programming of the self-similar equations, the local similarity equations, and auxiliary equations, respectively.

* Head, Aerodynamics and Heat Transfer Department. Associate Fellow AIAA.
† Member of Technical Staff. Member AIAA.

## I. Introduction

THE ratio of the local pressure on a body to the local pressure which would exist in an inviscid flow is a measure of the viscous interaction, that is, a measure of the degree to which the boundary layer influences the surface pressure, and therefore its own development. For the case of hypersonic flow over slender bodies with strong shock waves, the interaction depends on the ratio $\delta/r_w$.

The effect of viscous interaction on hypersonic flow over slender two-dimensional bodies has received considerable attention (e.g., Ref. 1). The corresponding problem for axisymmetric bodies has not been explored as thoroughly. A major difference between the two cases is that, for the latter, transverse curvature terms (whose magnitude also depend on $\delta/r_w$) must be retained in the boundary-layer equations. Hence, the boundary-layer solutions and techniques developed for two-dimensional flows are not directly applicable. Probstein and Elliott[2] have obtained boundary-layer solutions, including transverse curvature. Probstein[3] has applied these results to evaluate effects of transverse curvature on cones in the relatively weak interaction regime ($\delta/r_w \ll 1$). Yashuhara[4] has obtained solutions for self-similar flow over axisymmetric $\frac{3}{4}$-power-law bodies in the weak-to-moderate interaction regime [$\delta/r_w \lesssim O(1)$]. Stewartson[5] has treated the hypersonic flow of a model gas ($Pr = 1$, $\mu \sim T$) over very slender bodies and has obtained results that are valid in the limit of strong interaction ($\delta/r_w \to \infty$). More recently, Ellinwood and Mirels[6] have extended Stewartson's solution to nonmodel gases and have obtained the results in closed form.

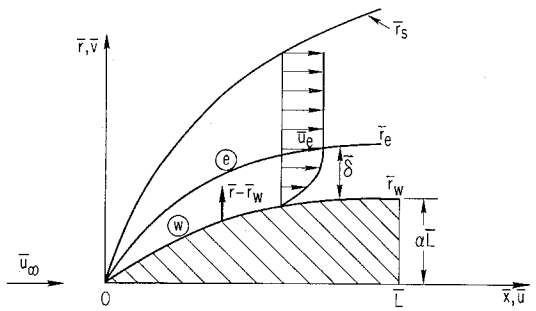


**Fig. 1 Coordinate system.**

No results have, as yet, been presented that span the entire range from weak-to-strong interaction for hypersonic flow over slender axisymmetric bodies. The primary object of this study is to obtain such solutions, assuming the shock is always strong. In particular, additional numerical results for $\frac{3}{4}$-power-law bodies are obtained. These are correlated and are then used to develop a local similarity method for finding hypersonic viscous interaction effects on slender axisymmetric bodies of arbitrary profile. Both two-dimensional and axisymmetric bodies are treated in a unified manner. Numerical results are presented for aerodynamic characteristics of a cone in the strong-to-weak interaction regimes.

The present study is a modified version of Ref. 7. The boundary-layer transformation is altered herein so that in the limit of strong interaction the local similarity solution is in agreement with the exact solution of Ref. 6. Further comparisons with Ref. 7 are noted in Appendix A.

## II. Analysis

### A. Equations of Motion

Consider hypersonic flow of a perfect gas past a slender two-dimensional or axisymmetric body. The boundary-layer displacement thickness is denoted by $\bar{\delta}^*$, the body ordinate by $\bar{r}_w$, the effective body ordinate by $\bar{r}_e = \bar{r}_w + \bar{\delta}^*$, and shock ordinate by $\bar{r}_s$ (Fig. 1). Assume that the shock slope is small, $(d\bar{r}_s/d\bar{x})^2 \ll 1$, and the freestream Mach number and shock strength are large, $(M_\infty d\bar{r}_s/d\bar{x})^2 \gg 1$, so that hypersonic small disturbance theory[1,8] can be used to evaluate the inviscid portion of the flowfield. Introduce the following nondimensionalization:

$$r = \bar{r}/\alpha\bar{L} \qquad x = \bar{x}/\bar{L} \qquad u = \bar{u}/\bar{u}_\infty$$
$$v = \bar{v}/\alpha\bar{u}_\infty \qquad p = \bar{p}/\alpha^2\bar{\rho}_\infty\bar{u}_\infty^2 \qquad \rho = \bar{\rho}/\bar{\rho}_\infty \quad (1)$$
$$h = 2\bar{h}/\bar{u}_\infty^2 \qquad H = 2\bar{H}/\bar{u}_\infty^2 \qquad \mu = \bar{\mu}/\bar{\mu}_\infty$$

where $\bar{L}$ is the body length and $\alpha$ is the characteristic body slope $\bar{r}_w(\bar{L})/\bar{L}$. If $(d\bar{r}_e/d\bar{x})^2 \ll 1$, the boundary-layer equations for a perfect gas become[2,4]

$$\rho u\frac{\partial u}{\partial x} + \rho v\frac{\partial u}{\partial r} = \rho_e u_e\frac{du_e}{dx} + \frac{1}{\alpha^2 Re}\frac{1}{r^\sigma}\frac{\partial}{\partial r}\left(\mu r^\sigma\frac{\partial u}{\partial r}\right) \quad (2a)$$

$$\partial\rho u/\partial x + (1/r^\sigma)(\partial\rho v r^\sigma/\partial r) = 0 \quad (2b)$$

$$p = [(\gamma - 1)/2\gamma](\rho h/\alpha^2) \quad (2c)$$

$$\rho u\frac{\partial H}{\partial x} + \rho v\frac{\partial H}{\partial r} = \frac{1}{\alpha^2 Re}\frac{1}{r^\sigma}\frac{\partial}{\partial r}\times$$
$$\left\{\frac{r^\sigma\mu}{Pr}\frac{\partial H}{\partial r} + \frac{(Pr - 1)}{Pr}r^\sigma\mu\frac{\partial u^2}{\partial r}\right\} \quad (2d)$$

where $Re = \bar{\rho}_\infty\bar{u}_\infty\bar{L}/\bar{\mu}_\infty$. Transformations used for the independent and dependent variables are

$$\frac{\xi}{[(\alpha\bar{L})^{\sigma+1}\bar{\rho}_\infty\bar{u}_\infty]^2} = \frac{\gamma M_\infty^2 C_w}{Re}\int_0^x u_e p_e r_e^{2\sigma}\,dx \quad (3a)$$

$$\frac{\eta}{(\alpha\bar{L})^{\sigma+1}\bar{\rho}_\infty\bar{u}_\infty} = \frac{u_e}{(2\xi)^{1/2}}\int_{r_w}^{r}\rho r^\sigma\,dr \quad (3b)$$

$$u/u_e = F_\eta(\xi,\eta) \quad (3c)$$

$$H/H_e = g(\xi,\eta) \quad (3d)$$

$$\rho v r^\sigma = \frac{-1}{(\alpha\bar{L})^{\sigma+1}\bar{\rho}_\infty\bar{u}_\infty}\left[\left(\frac{d\xi}{dx}\right)\frac{\partial(2\xi)^{1/2}F}{\partial\xi} + (2\xi)^{1/2}\frac{\partial\eta}{\partial x}\frac{\partial F}{\partial\eta}\right] \quad (3e)$$

The characteristic boundary-layer ordinate is taken to be $r_e$, rather than $r_w$, in Eq. (3a). (See Appendix A for further discussion.)

According to hypersonic small disturbance theory $u_e \doteq 1$, $h_e/H_e \doteq 2/[(\gamma - 1)M_e^2] \ll 1$ so that

$$\frac{\rho_e}{\rho} = \frac{H_e}{h_e}(g - F_\eta^2) + F_\eta^2 \doteq \frac{(\gamma - 1)M_e^2}{2}(g - F_\eta^2) \quad (4)$$

The equations of motion reduce to (assuming $\rho\mu = \rho_w\mu_w$)

$$(r_w/r_e)^{2\sigma}(R^\sigma F_{\eta\eta})_\eta + FF_{\eta\eta} + \beta(g - F_\eta^2) = 2\xi(F_\eta F_{\xi\eta} - F_\xi F_{\eta\eta}) \quad (5a)$$

$$F(\xi,0) = F_w \qquad F_\eta(\xi,0) = 0 \qquad F_\eta(\xi,\infty) = 1$$

$$\left(\frac{r_w}{r_e}\right)^{2\sigma}\left(\frac{R^\sigma}{Pr}g_\eta\right)_\eta + Fg_\eta + 2\left(\frac{r_w}{r_e}\right)^{2\sigma}\times\left(\frac{Pr - 1}{Pr}R^\sigma F_\eta F_{\eta\eta}\right)_\eta = 2\xi(F_\eta g_\xi - F_\xi g_\eta) \quad (5b)$$

$$g(\xi,0) = g_w \qquad g(\xi,\infty) = 1$$

$$R \equiv \left(\frac{r}{r_w}\right)^{\sigma+1} = 1 + B\int_0^\eta (g - F_\eta^2)\,d\eta \quad (5c)$$

where $R = R(\xi,\eta)$ and

$$\beta = \frac{-(\gamma - 1)}{\gamma}\frac{1}{p_e^2 r_e^{2\sigma}}\frac{dp_e}{dx}\int_0^x p_e r_e^{2\sigma}dx \quad (5d)$$

$$B = \frac{\sigma + 1}{2}(\gamma - 1)\left(\frac{2}{\gamma}\right)^{1/2}\frac{\Lambda}{p_e r_w^{\sigma+1}}\left(\int_0^x p_e r_e^{2\sigma}dx\right)^{1/2} \quad (5e)$$

$$\Lambda \equiv \frac{M_\infty}{\alpha^2}\left(\frac{C}{Re}\right)^{1/2} \quad (5f)$$

Here $C \equiv \bar{\mu}_m\bar{T}_\infty/\bar{\mu}_\infty\bar{T}_m$ and $\bar{T}_m$ is a suitable mean temperature to compensate for taking $\rho\mu = \rho_w\mu_w$ in Eqs. (5a) and (5b). Results from Refs. 6 and 9 suggest $\bar{T}_m/\bar{T}_0 = (g_{wi} + 3g_w)/6$.

Equations (3) and (5) contain the effective body ordinate $r_e$ defined by

$$\int_{r_w}^{r_e}\rho_e u_e r^\sigma dr = \int_{r_w}^{\infty}(\rho_e u_e - \rho u)r^\sigma dr$$

The latter equation can be expressed as

$$\left(\frac{r_e}{r_w}\right)^{\sigma+1} \equiv R(\xi,\infty) = 1 + B\int_0^\infty (g - F_\eta^2)d_\eta \equiv 1 + BJ_e \quad (6)$$

Since $R(\xi,\eta)$ approaches a finite value as $\eta \to \infty$, $\delta$ has a finite value and is equal to $\delta^*$. Thus $r_e$ can be considered to be the value of $r$ at the outer edge of the boundary layer as well as the effective body ordinate. This is due to the simplified form for $\rho_e/\rho$ introduced in Eq. (4) (i.e., this assumption becomes invalid at the edge of the boundary layer).

A suitable expression relating $p_e$ and $r_e$ is now needed. Write

$$p_e = k^2 \dot{r}_e^2 \tag{7a}$$

The coefficient $k$ is independent of $x$ for effective bodies that follow a power law, $r_e \sim x^{m_e}$.[8] Values of $k$ and a quantity defining shock location $\zeta \equiv r_e/r_s$ are given in Table 1a for specified values of $\gamma$, $\sigma$, and $m_e$. For bodies that do not grow as a power of $x$, $k$ may be approximated by

$$k^2 = k_1^2\left[1 + k_2\left(\frac{m_e - 1}{(\sigma + 1)m_e}\right) + k_3\left(\frac{m_e - 1}{(\sigma + 1)m_e}\right)^2 + \ldots\right] \tag{7b}$$

where $m_e$ is a "local" power-law exponent defined by

$$(m_e - 1)/m_e \equiv r_e\ddot{r}_e/\dot{r}_e^2 \tag{7c}$$

and where $k_1$, $k_2$, and $k_3$ are functions of $\gamma$ and $\sigma$. The choice $k_2 = k_3 = 0$ corresponds to a tangent wedge or tangent cone approximation, whereas $k_1 = k_2 = 1$ and $k_3 = 0$ correspond to a Newtonian approximation. The values of $k_1$, $k_2$, and $k_3$ in Table 1b have been chosen to match the exact value of $k$ for power-law bodies with exponents $m_e = 1$ and $\frac{3}{4}$ (for $\sigma = 1$) and $m_e = 1$, $\frac{6}{7}$, and $\frac{3}{4}$ (for $\sigma = 0$). The use of these values of $k_1$, $k_2$, and $k_3$ is expected to be accurate for arbitrary body shapes when the local values of $m_e$ are in the range $\frac{3}{4} \leq m_e \leq 1$ (which is the range of major interest herein). When $m_e \leq 2/(\sigma + 3)$, the local pressure is no longer related to the local value of $r_e$, but is determined primarily by nose bluntness.[7,8] These cases, as well as entropy layer effects, are excluded from present consideration. Equations (7) are consistent with the use of local similarity introduced in later sections. A similar development can be made to estimate local values of $\zeta$ for bodies other than power laws. This is not done since $\zeta$ does not vary significantly with $m_e$ for $\sigma = 1$ and $\frac{3}{4} \leq m_e \leq 1$ (Table 1).

Equations (5–7) define the boundary-layer development. Shear and heat transfer are found from

$$\tau_w \equiv \frac{\bar{\tau}_w}{\alpha^3 \bar{\rho}_\infty \bar{u}_\infty{}^2} = \left(\frac{\gamma}{2}\right)^{1/2} \times \Lambda\left[r_w{}^\sigma p_e (F_{\eta\eta})_w \Big/ \left(\int_0^x p_e r_e{}^{2\sigma} dx\right)^{1/2}\right] \tag{8a}$$

$$\mathfrak{q}_w \equiv \frac{Pr}{\alpha^3 \bar{\rho}_\infty \bar{u}_\infty \bar{H}_\infty} \bar{q}_w = \left(\frac{\gamma}{2}\right)^{1/2} \times \Lambda\left[r_w{}^\sigma p_e (g_\eta)_w \Big/ \left(\int_0^x p_e r_e{}^{2\sigma} dx\right)^{1/2}\right] \tag{8b}$$

For cases where the effective body can be approximated by a power law, Eqs. (5) indicate

$$\beta = [(\gamma - 1)/\gamma]\{2(1 - m_e)/[2(\sigma + 1)m_e - 1]\} \tag{9a}$$

$$B = \frac{(\sigma + 1)(\gamma - 1)}{m_e k (2\gamma)^{1/2}[2(\sigma + 1)m_e - 1]^{1/2}} \frac{\Lambda x^{3/2}}{r_w{}^{1+\sigma} r_e{}^{1-\sigma}} \tag{9b}$$

$\beta$ is constant and generally small (particularly for $\sigma = 1$). If the physical body is a power law, $r_w \sim x^m$, then $B \sim x^{3/2+\sigma(m_e-m)-(m_e+m)}$. When $m = \frac{3}{4}$, it can be shown that $m_e = \frac{3}{4}$ for all $x$. Hence $B$ is a constant and Eqs. (5) become independent of $\xi$. This case corresponds to self-similar flow and is discussed in the next section. When $m > \frac{3}{4}$, it can be shown that $m_e \to \frac{3}{4}$, $B \to \infty$ as $x \to 0$ and that $m_e \to m$, $B \to 0$ as $x \to \infty$. Hence the interaction is strong at the leading edge and decreases with downstream distance. When $m < \frac{3}{4}$, it can be shown that $m_e \to m$, $B \to 0$ as $x \to 0$ and that $m_e \to \frac{3}{4}$, $B \to \infty$ as $x \to \infty$. Thus the interaction is weak at the leading edge and increases with downstream distance.

The quantity $\beta$ in Eqs. (5) is the usual local pressure gradient parameter. The quantity $B$ is a measure of the local value of $(r_e/r_w)^{\sigma+1}$. For $\sigma = 0$, Eqs. (5a) and (5b) are independent of $R$, regardless of the value of $B$. The dependence of Eqs. (5a) and (5b) on $R$ for $\sigma = 1$ is referred to as the "transverse curvature" effect.

Equations (5) indicate that for a given normalized body shape $r_w$ the variation of dependent variables with $x$ depends on $\gamma$, $P_r$, $g_w$, $F_w$ and $\Lambda$, where $\Lambda$ is a measure of the magnitude of $B$ and therefore of $(r_e/r_w)^{\sigma+1}$. The quantity $\Lambda$ is referred to herein as the "interaction parameter."‡

**Table 1 Pressure and shock location**

a) Effective bodies with power-law shape, $r_e \sim x^{m_e}$

| | | $\sigma = 0$ | | $\sigma = 1$ | |
|---|---|---|---|---|---|
| $m_e$ | $\gamma$ | $\zeta = r_e/r_s$ | $k^2$ | $\zeta = r_e/r_s$ | $k^2$ |
| 1 | 1.00 | 1.0000 | 1.0000 | 1.0000 | 1.0000 |
| | 1.15 | 0.9302 | 1.0750 | 0.9649 | 1.0180 |
| | 1.40 | 0.8333 | 1.2000 | 0.9149 | 1.0450 |
| | $\frac{5}{3}$ | 0.7500 | 1.3333 | 0.8704 | 1.0708 |
| $\frac{3}{4}$ | 1.00 | 1.0000 | 0.6667 | 1.0000 | 0.8333 |
| | 1.15 | 0.7800 | 0.9691 | 0.9447 | 0.8685 |
| | 1.40 | 0.5912 | 1.4214 | 0.8751 | 0.9116 |
| | $\frac{5}{3}$ | 0.4793 | 1.8588 | 0.8192 | 0.9455 |

b) Coefficients for Eq. (7b)

| | $\sigma = 0$ | | | $\sigma = 1$ | | |
|---|---|---|---|---|---|---|
| $\gamma$ | $k_1^2$ | $k_2$ | $k_3$ | $k_1^2$ | $k_2$ | $k_3$ |
| 1.00 | 1.000 | 1.000 | 0.0 | 1.000 | 1.000 | 0 |
| 1.15 | 1.075 | 1.004 | 2.125 | 1.018 | 0.881 | 0 |
| 1.40 | 1.200 | 0.993 | 4.639 | 1.045 | 0.766 | 0 |
| $\frac{5}{3}$ | 1.333 | 0.980 | 6.487 | 1.071 | 0.703 | 0 |

## B. Self-Similar Flow

Consider a body defined by $r_w = x^{3/4}$. As pointed out in Ref. 4, $r_e \sim x^{3/4}$, $\beta$ and $B$ are constant, Eqs. (5) are functions only of $\eta$, and the flow is self-similar at each axial station. Equation (5) with derivatives of $\xi$ neglected can then be solved for $J_e$, $F''_w$, and $g'_w$ corresponding to given values of $\beta$, $P_r$, $B$, $F_w$ and $g_w$. These quantities define the boundary-layer thickness, pressure, shear, and heat transfer. Thus, collecting the equations of interest, $\beta = (\gamma - 1)/[\gamma(3\sigma + 1)]$ and

$$\Lambda = (3k/4)[\gamma^{1/2}/(\gamma - 1)](r_e/r_w)^{1-\sigma} B \tag{10a}$$

$$x^{1/2} p_e = [(3k/4)(r_e/r_w)]^2 \tag{10b}$$

$$x^{3/4}\tau_w = [(\sigma + 1)/2](\gamma - 1)\Lambda^2(F''_w/B) \tag{10c}$$

$$x^{3/4} q_w = [(\sigma + 1)/2](\gamma - 1)\Lambda^2(g'_w/B) \tag{10d}$$

$$\frac{C_D}{(C_D)_{\text{in}}} = \left(\frac{r_e}{r_w}\right)^2\left[1 + \frac{\sigma + 1}{3}\frac{2\gamma}{\gamma - 1}\left(\frac{r_w}{r_e}\right)^{2\sigma} BF''_w\right] \tag{10e}$$

where

$$r_e/r_w = (1 + BJ_e)^{1/(\sigma+1)} \tag{10f}$$

Since $\Lambda$ is expressed directly in terms of body geometry and freestream conditions, it is convenient to consider Eqs. (10) as parametric equations (with $B$ as the parameter) relating the dependent variables to $\Lambda$.

Numerical solutions of the self-similar equations for $B \neq 0$ have been presented in Refs. 4, 6, and 7 using dependent and independent variables that differ from those used here (see Appendix A). Some of these results are given in Table 2. Results for $Pr = 0.7$; $\beta = 0$, $\frac{1}{14}$; $g_w = 0$, 0.2; $g'_w = 0$; $0 \leq (r_w/r_e)^\sigma B \leq 10^5$; and $F_w = 0$, $-0.4$ are included. The case $F_w = -0.4$ corresponds to surface blowing and is not pursued in later sections. The quantity $A$ appearing in Table 2 is the transverse curvation parameter used in Ref. 7

‡ Recall that for hypersonic flow over two-dimensional as well as axisymmetric slender bodies, with strong shock waves, the ratio $r_e/r_w$ defines the degree of viscous interaction, i.e., the degree to which the local pressure departs from the value for inviscid flow.

**Table 2 Numerical solutions of self-similar boundary-layer equations for $Pr = 0.7$, $\rho\mu = \rho_w\mu_w{}^a$**

| | | | | | | | | $\gamma = 1.4$, $\sigma = 1$ | | |
|---|---|---|---|---|---|---|---|---|---|---|
| $F_w$ | $\beta$ | $g_w$ | $(r_w/r_e)^\sigma B = A$ | $(r_w/r_e)^\sigma g'_w$ | $(r_w/r_e)^\sigma F''_w$ | $(r_e/r_w)^\sigma J_e$ | $(1 + BJ_e)^{1/2} = (r_e/r_w)^{(\sigma+1)/2}$ | $\Lambda$ | $\frac{C_D}{(C_D)_{in}}$ | $\frac{x^{1/4}\,Kn}{\alpha(g_w)^{1/2}\Lambda}$ |
| 0 | 0[b] | 0 | 0 | $3.459^{-1}$ | $4.696^{-1}$ | $4.019^{-1}$ | | | | |
| | | 0.15 | 0 | $2.838^{-1}$ | $4.696^{-1}$ | $6.097^{-1}$ | | | | |
| | | 0.40 | 0 | $1.804^{-1}$ | $4.696^{-1}$ | $9.560^{-1}$ | | | | |
| | | 0.60 | 0 | $9.756^{-2}$ | $4.696^{-1}$ | 1.233 | | | | |
| | | 0.8357 | 0 | 0 | $4.696^{-1}$ | 1.559 | | | | |
| | 0[c] | 0 | 1 | $3.724^{-1}$ | $5.060^{-1}$ | $4.360^{-1}$ | 1.198 | $2.53\bar{5}$ | 4.827 | |
| | | | 5 | $4.681^{-1}$ | $6.377^{-1}$ | $5.596^{-1}$ | 1.949 | $2.061^{+1}$ | $5.652^{+1}$ | |
| | | | 10 | $5.736^{-1}$ | $7.830^{-1}$ | $6.95\bar{5}^{-1}$ | 2.820 | $5.961^{+2}$ | $2.986^{+2}$ | |
| | | | 50 | 1.228 | 1.686 | 1.544 | 8.842 | $9.352^{+2}$ | $3.084^{+4}$ | |
| | | | $10^2$ | 1.889 | 2.599 | 2.404 | $1.554^{+1}$ | $3.286^{+3}$ | $2.930^{+5}$ | |
| | | | $10^3$ | $1.021^{+1}$ | $1.414^{+1}$ | $1.336^{+1}$ | $1.156^{+2}$ | $2.445^{+5}$ | $8.819^{+8}$ | |
| | | 1 | 0 | $-6.8^{-2}$ | $4.696^{-1}$ | 1.79 | 1 | | | |
| | | | 5 | $-2.29^{-1}$ | 1.255 | 3.76 | 4.450 | | | |
| | | | 10 | $-3.60^{-1}$ | 1.846 | 5.25 | 7.314 | | | |
| 0 | $\frac{1}{14}$[d] | 0 | 0 | $3.482^{-1}$ | $4.871^{-1}$ | $3.743^{-1}$ | 1 | 0 | 1 | 0.3812 |
| | | | 0.5 | $3.610^{-1}$ | $5.050^{-1}$ | $3.895^{-1}$ | 1.093 | 1.156 | 2.603 | 0.3616 |
| | | | 1 | $3.735^{-1}$ | $5.224^{-1}$ | $4.034^{-1}$ | $1.18\bar{5}$ | 2.506 | 4.824 | 0.3451 |
| | | | 2.5 | $4.096^{-1}$ | $5.727^{-1}$ | $4.456^{-1}$ | 1.454 | 7.688 | $1.624^{+1}$ | 0.3083 |
| | | | 5 | $4.657^{-1}$ | $6.510^{-1}$ | $5.109^{-1}$ | 1.885 | $1.994^{+1}$ | $5.754^{+1}$ | 0.2703 |
| | | | 7.5 | $5.182^{-1}$ | $7.242^{-1}$ | $5.713^{-1}$ | 2.299 | $3.647^{+1}$ | $1.392^{+2}$ | 0.2466 |
| | | | 10 | $5.678^{-1}$ | $7.935^{-1}$ | $6.228^{-1}$ | 2.700 | $5.710^{+1}$ | $2.772^{+2}$ | 0.2300 |
| | | | 15 | $6.612^{-1}$ | $9.238^{-1}$ | $7.353^{-1}$ | 3.468 | $1.100^{+2}$ | $7.900^{+2}$ | 0.2085 |
| | | | 20 | $7.486^{-1}$ | 1.046 | $8.375^{-1}$ | 4.213 | $1.782^{+2}$ | $1.750^{+3}$ | 0.1943 |
| | | | 50 | 1.205 | 1.684 | 1.368 | 8.330 | $8.809^{+2}$ | $2.733^{+4}$ | 0.1583 |
| | | | $10^2$ | 1.851 | 2.587 | 2.117 | $1.458^{+1}$ | $3.084^{+3}$ | $2.569^{+5}$ | 0.1389 |
| | | | $5\cdot10^2$ | 5.831 | 8.163 | 6.774 | $5.821^{+1}$ | $6.156^{+4}$ | $6.454^{+7}$ | 0.1097 |
| | | | $10^3$ | 9.992 | $1.400^{+1}$ | $1.165^{+1}$ | $1.080^{+2}$ | $2.284^{+5}$ | $7.614^{+8}$ | 0.1015 |
| | | | $10^4$ | $6.698^{+1}$ | $9.505^{+1}$ | $7.904^{+1}$ | $8.891^{+2}$ | $1.880^{+7}$ | $3.469^{+12}$ | 0.08280 |
| | | | $10^5$ | $4.998^{+2}$ | $7.030^{+2}$ | $5.944^{+2}$ | $7.710^{+3}$ | $1.631^{+9}$ | $1.9\bar{5}0^{+16}$ | 0.07137 |
| | | 0.2 | 0 | $2.657^{-1}$ | $5.016^{-1}$ | $6.353^{-1}$ | 1 | 0 | 1 | 0.3926 |
| | | | 1 | $3.034^{-1}$ | $5.726^{-1}$ | $7.094^{-1}$ | 1.307 | 2.765 | 6.277 | 0.3429 |
| | | | 5 | $4.299^{-1}$ | $8.114^{-1}$ | $9.637^{-1}$ | 2.412 | $2.551^{+1}$ | $1.160^{+2}$ | 0.2633 |
| | | | 10 | $5.623^{-1}$ | 1.062 | 1.235 | 3.654 | $7.729^{+1}$ | $6.751^{+2}$ | 0.2275 |
| | | | 20 | $7.901^{-1}$ | 1.494 | 1.708 | 5.929 | $2.508^{+2}$ | $4.937^{+3}$ | 0.1972 |
| | | | 50 | 1.357 | 2.572 | $2.89\bar{5}$ | $1.207^{+1}$ | $1.277^{+3}$ | $8.761^{+4}$ | 0.1668 |
| | | | $10^2$ | 2.156 | 4.094 | 4.576 | $2.141^{+1}$ | $4.530^{+3}$ | $8.766^{+5}$ | 0.1497 |
| | | | $5\cdot10^2$ | 7.124 | $1.359^{+1}$ | $1.512^{+1}$ | $8.694^{+1}$ | $9.195^{+4}$ | $2.398^{+8}$ | 0.1224 |
| | | | $10^3$ | $1.236^{+1}$ | $2.363^{+1}$ | $2.62\bar{5}^{+1}$ | $1.620^{+2}$ | $3.427^{+5}$ | $2.894^{+9}$ | 0.1142 |
| | | | $10^4$ | $8.498^{+1}$ | $1.633^{+2}$ | $1.812^{+2}$ | $1.346^{+3}$ | $2.847^{+7}$ | $1.381^{+13}$ | 0.09497 |
| | | $8.308^{-1}$ | 0 | 0 | $5.464^{-1}$ | 1.443 | 1 | 0 | 1 | 0.4277 |
| | | $8.166^{-1}$ | 1 | 0 | $7.183^{-1}$ | 1.746 | 1.657 | 3.505 | $1.195^{+1}$ | 0.3393 |
| | | $7.984^{-1}$ | 5 | 0 | 1.229 | 2.691 | 3.802 | $4.021^{+1}$ | $4.288^{+1}$ | 0.2530 |
| | | $7.904^{-1}$ | 10 | 0 | 1.738 | $3.65\bar{5}$ | 6.128 | $1.296^{+2}$ | $3.083^{+3}$ | 0.2220 |
| | | $7.831^{-1}$ | 20 | 0 | $2.60\bar{5}$ | 5.296 | $1.034^{+1}$ | $4.374^{+2}$ | $2.610^{+4}$ | 0.1972 |
| | | $7.751^{-1}$ | 50 | 0 | 4.768 | 9.396 | $2.170^{+1}$ | $2.295^{+3}$ | $5.242^{+5}$ | 0.1720 |
| | | $7.700^{-1}$ | $10^2$ | 0 | 7.841 | $1.520^{+1}$ | $3.900^{+1}$ | $8.250^{+3}$ | $5.568^{+6}$ | 0.1574 |
| | | $7.609^{-1}$ | $5\cdot10^2$ | 0 | $2.729^{+1}$ | $5.166^{+1}$ | $1.607^{+2}$ | $1.700^{+5}$ | $1.645^{+9}$ | 0.1329 |
| | | $7.578^{-1}$ | $10^3$ | 0 | $4.805^{+1}$ | $9.037^{+1}$ | $3.006^{+2}$ | $6.358^{+5}$ | $2.026^{+10}$ | 0.1251 |
| | | $7.501^{-1}$ | $10^4$ | 0 | $3.409^{+2}$ | $6.321^{+2}$ | $2.514^{+3}$ | $5.318^{+7}$ | $1.006^{+14}$ | 0.1061 |
| | | $7.447^{-1}$ | $10^5$ | 0 | $2.624^{+3}$ | $4.819^{+3}$ | $2.195^{+4}$ | $4.643^{+9}$ | $5.901^{+17}$ | 0.09355 |
| −0.4 | $\frac{1}{14}$ | 0 | 0 | $1.690^{-1}$ | $2.230^{-1}$ | $4.700^{-1}$ | 1 | 0 | 1 | |
| | | | 1 | $1.983^{-1}$ | $2.632^{-1}$ | $5.036^{-1}$ | 1.226 | 2.594 | 3.350 | |
| | | | 5 | $2.992^{-1}$ | $4.022^{-1}$ | $6.191^{-1}$ | 2.024 | $2.141^{+1}$ | $4.256^{+1}$ | |
| | | | 10 | $4.066^{-1}$ | $5.509^{-1}$ | $7.429^{-1}$ | 2.903 | $6.141^{+1}$ | $2.251^{+2}$ | |
| | | | 50 | 1.054 | 1.453 | 1.491 | 8.691 | $9.191^{+2}$ | $2.569^{+4}$ | |
| | | | $10^2$ | 1.703 | 2.360 | 2.248 | $1.503^{+1}$ | $3.178^{+3}$ | $2.489^{+5}$ | |

[a] Note, $3.4^{-1} = 3.4 \times 10^{-1}$, etc.
[b] Ref. 12.
[c] Ref. 4.
[d] Present results.

and, for self-similar flows, is related to $B$ by $A = (r_w/r_e)^\sigma B$. Hence $A$ and $B$ can be used interchangeably.

Boundary-layer parameters of interest have been correlated in Ref. 7 for $Pr = 0.7$ and $F_w = 0$. In present notation, these correlations§ can be expressed as

$$BJ_e = I_{e00}(1 + \beta I_\beta)\left[1 + \frac{\sigma I_1 A}{1 + I_2 \ln(1 + I_3 A)}\right] A \quad (11a)$$

$$\left(\frac{r_w}{r_e}\right)^\sigma F''_w = F''_{w00}(1 + \beta F_\beta) \times \left[1 + \frac{\sigma F_1 A}{1 + F_2 \ln(1 + F_3 A)}\right] \quad (11b)$$

$$\left(\frac{r_w}{r_e}\right)^\sigma \frac{g'_w}{g_{wi} - g_w} = G'_{w00}(1 + \beta G_\beta) \times \left[1 + \frac{\sigma G_1 A}{1 + G_2 \ln(1 + G_3 A)}\right] \quad (11c)$$

§ Attempts were made to obtain new correlations in terms of $B$ rather than $A$. These did not have the same accuracy for large $B$ as the correlations of Ref. 7.

**Table 3 Coefficients for correlation of numerical solutions of $\beta = \frac{1}{14}$, $F_w = 0$, $Pr = 0.7$ cases [Eqs. (11)]**

| $g_w$ | $g'_w$ | $I_1$ | $I_2$ | $I_3$ | $F_1$ | $F_2$ | $F_3$ | $G_1$ | $G_2$ | $G_3$ |
|---|---|---|---|---|---|---|---|---|---|---|
| 0 | ... | 0.07933 | 0.3717 | 0.05654 | 0.07405 | 0.3594 | 0.06378 | 0.09624 | 0.3674 | 0.1575 |
| 0.2 | ... | 0.1211 | 0.3870 | 0.1076 | 0.1480 | 0.4211 | 0.1163 | 0.1787 | 0.4407 | 0.1577 |
| | 0 | 0.2262 | 0.4677 | 0.1763 | 0.3458 | 0.5118 | 0.2140 | ... | ... | ... |

$$g_{wi} = 0.8357(1 - 0.082\beta) \times \left(1 - \frac{0.1576\sigma}{1 + 5.04/[\ln(1 + 0.847A)]}\right) \quad (11d)$$

where

$$I_{e00} = 0.4019(1 + 3.46g_w) \quad (12a)$$

$$F''_{w00} = 0.4696 \quad (12b)$$

$$G'_{w00} = 0.4139 \quad (12c)$$

$$I_\beta = -0.96 \qquad F_\beta = 0.52(1 + 4.1g_w)$$
$$G_\beta = 0.18(1 + 2.0g_w) \quad (12d)$$

If the variables $I_e \equiv BJ_e/A$, $(r_w/r_e)^\sigma F''_w$, $(r_w/r_e)^\sigma g'_w$, and $g_{wi}$ are denoted by $\psi(\beta,A)$, then the first factor on the right-hand side of Eqs. (11) corresponds to $\psi(0,0)$; the second factor corresponds to $\psi(\beta,0)/\psi(0,0)$ and corrects for $\beta \neq 0$, $A = 0$. The third factor corresponds to $\psi(\beta,A)/\psi(\beta,0)$ and corrects for effect of $A$ at constant $\beta$. The coefficients for the latter factor are based on the $\beta = \frac{1}{14}$ solution and are given in Table 3. These coefficients have been chosen to match the $\beta = \frac{1}{14}$ solution at $A = 1$, 10, and 100 and they correlate this solution to within fractions of a percent for $A \leq 100$, to within 4% for $A \leq 500$, and to within 7% for $A \leq 1000$. The quantity $g_{wi}$ in Eq. (11d) is the insulated wall value of $g_w$ as a function of $\beta$ and $A$. Note, $g_{wi} \doteq (Pr)^{1/2}$ for $A = \beta = 0$ and, as will be shown, $g_{wi} \to Pr$ as $A \to \infty$.

The closed-form solution in Ref. 6 for hypersonic flow over slender axisymmetric bodies is valid in the limit $A \to \infty$. In the case of $\frac{3}{4}$-power-law bodies, the results for $F''_w$, $g'_w$, and $J_e$ can be expressed as

$$\left(\frac{r_w}{r_e}\right) F''_w = \left(\frac{r_w}{r_e}\right) \frac{g'_w}{Pr - g_w} = \frac{Pr + 3g_w}{12} \frac{A}{\ln A} [1 + 0(\ln^{-1/2} A)] \quad (13a)$$

$$BJ_e = \frac{2\gamma}{3\gamma - 1} \frac{Pr + g_w}{Pr} \frac{Pr + 3g_w}{12} \frac{A^2}{\ln A} \times [1 + 0(\ln^{-1/2} A)] \quad (13b)$$

The convergence to the limit $A \to \infty$ is very slow. Note that Eqs. (11) have the proper dependence on $A$ as $A \to \infty$. Equation (13a) confirms that $g_{wi} = Pr$ for $A \to \infty$.

### C. Local Similarity Solutions

In order to obtain a solution for the viscous flow over arbitrary bodies, the following equations must be solved simultaneously for $r_e$, $p_e$, $B$, and $\beta$ as functions of $x$:

$$(r_e/r_w)^{\sigma+1} = 1 + BJ_e \quad (14a)$$

$$p_e = k^2 \dot{r}_e^2 \quad (14b)$$

$$\left(\frac{r_w}{r_e}\right)^\sigma B = \frac{\sigma + 1}{2} \left(\frac{2}{\gamma}\right)^{1/2} (\gamma - 1) \times \frac{\Lambda}{p_e r_w r_e^\sigma} \left(\int_0^x p_e r_e^{2\sigma} dx\right)^{1/2} \quad (14c)$$

$$\beta = \frac{-(\gamma - 1)}{\gamma} \frac{1}{p_e^2 r_e^{2\sigma}} \frac{dp_e}{dx} \int_0^x p_e r_e^{2\sigma} dx \quad (14d)$$

In principle, $J_e$ must be obtained from a numerical solution of the nonsimilar boundary-layer equations (5). However, if it is assumed that $J_e$ depends only on the local values of $(\beta,B)$, then a knowledge of $J_e(\beta,B)$ from the self-similar flow equations permits Eqs. (14a–14d) to be evaluated independent of the nonsimilar boundary-layer equations. Similarly, the local values of $(F_{\eta\eta})_w$ and $(g_\eta)_w$ can be assumed to depend only on the local values of $(\beta,B)$ so that the self-similar solutions for $F''_w$ and $g'_w$ are also applicable. This approach is termed a local similarity approximation and generally gives good agreement with exact solutions of the nonsimilar equations. The local similarity solution is exact in the limit $\sigma = 0$, $\gamma \to 1$ and agrees with Cheng's method[9] for this limit. It is also exact in the limits of "no" interaction on a power-law body and, as will be shown, for strong interaction on an arbitrary body.

The local similarity solution of Eqs. (14) requires a knowledge of $BJ_e$ (as a function of $B,\beta$) from the self-similar flow equations. Equation (11a) provides this information. Since Eq. (11a) contains $A$ rather than $B$, it is convenient to eliminate either $A$ or $B$ from this system of equations. Recall that for self-similar flows

$$A = B(r_w/r_e)^\sigma = B(1 + BJ_e)^{-\sigma/(\sigma+1)}$$

These equations also apply for locally self-similar flows since $x$ does not appear explicitly. Substitution of $A$ for $B(r_w/r_e)^\sigma$ in Eq. (14c) and use of Eq. (11a) then replaces $B$ by $A$ as the transverse curvature parameter. Equation (14) will be used to evaluate weak interaction over a cone and strong interaction over arbitrary bodies. The numerical solution of Eq. (14) will then be discussed.

#### 1. *Weak interaction*

The local similarity solution for a cone in the weak interaction region [using Eq. (7) with $k_3 = 0$] is

$$\begin{aligned} \delta/r_w &= \delta_1\Lambda_x [1 + \delta_2\Lambda_x + \dots] \\ A &= A_1\Lambda_x [1 + A_2\Lambda_x + \dots] \\ [p_e/(p_e)_{in}] - 1 &= p_1\Lambda_x + p_2\Lambda_x^2 + \dots \\ \tau_w &= \tau_1\Lambda_x [1 + \tau_2\Lambda_x + \dots] \\ \frac{q_w}{g_{wi} - g_w} &= q_1\Lambda_x [1 + q_2\Lambda_x + \dots] \\ \beta &= \beta_1\Lambda_x [1 + \dots] \\ \frac{C_D}{(C_D)_{in}} - 1 &= C_1\Lambda_x + C_2\Lambda_x^2 + \dots \end{aligned} \quad (15)$$

where $\Lambda_x \equiv \Lambda/(x)^{1/2}$ is the local value of the interaction parameter and

$$\delta_1 = \frac{\gamma - 1}{k_1} \frac{I_{e00}}{(6\gamma)^{1/2}}$$

$$\frac{\delta_2}{\delta_1} = \frac{\gamma - 1}{6\gamma} \left(1 - \frac{k_2}{8}\right) I_\beta + \frac{2I_1}{I_{e00}} - \frac{7}{10} + \frac{k_2}{20}$$

$$A_1/\delta_1 = 2/I_{e00} \qquad A_2/\delta_1 = -\tfrac{1}{5}[1 - (k_2/4)]$$

$$\frac{p_1}{\delta_1} = 1 - \left(\frac{k_2}{8}\right) \qquad \frac{p_2}{\delta_1^2} = \frac{1}{4}\left[1 - \frac{k_2}{2}\right]$$

**Table 4 Constants defining weak interaction for cone [Eqs. (15)] $Pr = 0.7$**

| $\gamma$ | $g_w$ | $\delta_1$ | $(-1)\delta_2$ | $C_1$ | $C_2$ | $p_1$ | $p_2 \times 10^3$ | $\tau_1$ | $\tau_2$ | $q_1$ | $q_2$ |
|---|---|---|---|---|---|---|---|---|---|---|---|
| 1.4 | 0.0 | 0.05426 | 0.01673 | 0.9530 | 0.04083 | 0.04906 | 0.4541 | 0.6957 | 0.02998 | 0.6132 | 0.03518 |
| | 0.2 | 0.09181 | 0.03184 | 0.9983 | 0.08055 | 0.08302 | 1.300 | 0.6957 | 0.05855 | 0.6132 | 0.06409 |
| | 0.836 | 0.2112 | 0.08741 | 1.142 | 0.2114 | 0.1910 | 6.881 | 0.6957 | 0.1485 | 0.6132 | 0.1319 |
| $\frac{5}{3}$ | 0.0 | 0.08187 | 0.02689 | 1.056 | 0.06855 | 0.07468 | 1.087 | 0.7684 | 0.04626 | 0.6773 | 0.05360 |
| | 0.2 | 0.1385 | 0.05085 | 1.125 | 0.1370 | 0.1264 | 3.111 | 0.7684 | 0.09111 | 0.6773 | 0.09776 |
| | 0.836 | 0.3187 | 0.1383 | 1.344 | 0.3745 | 0.2907 | 16.47 | 0.7684 | 0.2380 | 0.6773 | 0.2027 |

$$\frac{\tau_1}{\delta_1} = \frac{3\gamma k_1^2}{\gamma - 1}\frac{F''_{w00}}{I_{e00}}$$

$$\frac{\tau_2}{\delta_1} = \frac{\gamma - 1}{6\gamma}\left[1 - \frac{k_2}{8}\right]F_\beta + \frac{2F_1}{I_{e00}} + \frac{1}{5}\left[1 - \frac{k_2}{4}\right] \quad (16)$$

$$\frac{q_1}{\delta_1} = \frac{3\gamma k_1^2}{\gamma - 1}\frac{G'_{w00}}{I_{e00}}$$

$$\frac{q_2}{\delta_1} = \frac{\gamma - 1}{6\gamma}\left[1 - \frac{k_2}{8}\right]G_\beta + \frac{2G_1}{I_{e00}} + \frac{1}{5}\left[1 - \frac{k_2}{4}\right]$$

$$\frac{C_1}{\delta_1} = \frac{4}{3}\left[1 - \frac{k_2}{8} + \frac{3\gamma}{\gamma - 1}\frac{F''_{w00}}{I_{e00}}\right]$$

$$\frac{C_2}{\delta_1^2} = \frac{1}{2}\left[1 - \frac{k_2}{2}\right]\left[1 + \frac{\tau_1\tau_2}{k_1^2 p_2}\right]$$

$$\beta_1/\delta_1 = [(\gamma - 1)/6\gamma][1 - (k_2/8)]$$

When $Pr = 0.7$ and $\gamma = 1.4$

$$g_{wi}/0.8357 = 1 - 0.00735\Lambda_x[1 + 0.091 g_w] + 0(\Lambda_x^2)$$

and $g_{wi}$ departs only slightly from 0.8357. The small dependence of $g_{wi}$ on $g_w$ is due to the effect of the latter on $\beta$ and $A$. Values of the coefficients in Eqs. (15) are given in Table 4 for $\gamma = 1.4, \frac{5}{3}$ and $Pr = 0.7$. Transverse curvature effects are associated with the terms $F_1$, $G_1$, and $I_1$ in Eqs. (16).

### 2. *Strong interaction*

We now consider bodies in the limit $\Lambda_x \gg 1$. It can be shown¶ that to leading order $r_e \sim \delta \sim x^{3/4}$. It then follows that $m_e = \frac{3}{4}$ and from Eqs. (9)

$$\beta = (\gamma - 1)/[\gamma(3\sigma + 1)] \quad (17a)$$

$$\Lambda_x \equiv \frac{\Lambda x^{3/2}}{r_w^2} = \frac{3k}{4}\frac{(\gamma)^{1/2}}{\gamma - 1}A(BJ_e)^{1/(\sigma+1)} \quad (17b)$$

Equation (17b) defines the local values of $x$ that correspond to given values of $(A,\beta)$. The assumption of local similarity then permits all boundary-layer properties to be evaluated at that station.

Consider axisymmetric bodies. If Eqs. (13) are used to relate $BJ_e$, $F''_w$, and $g'_w$ to $(A,\beta)$, it is found that for $\sigma = 1$, $\Lambda_x \gg 1$

$$\frac{x^{-3/4}\delta}{\Lambda^{1/2}} = \frac{2}{3}\left[\frac{\gamma - 1}{k}\right]^{1/2} \times \left[\frac{3}{3\gamma - 1}\frac{(Pr + g_w)(Pr + 3g_w)}{Pr}\frac{1}{\ln\Lambda_x}\right]^{1/4} \times [1 + 0(\ln^{-1/2}\Lambda_x)] \quad (18a)$$

$$\frac{x^{1/2}p_e}{\Lambda} = \frac{9k^2}{16}\left[\frac{x^{-3/4}\delta}{\Lambda^{1/2}}\right]^2 \quad (18b)$$

$$\frac{r_w\tau_w}{\Lambda^2} = \frac{r_w}{\Lambda^2}\frac{q_w}{Pr - g_w} = (\gamma - 1)\frac{(Pr + 3g_w)}{6}\frac{1}{\ln\Lambda_x}[1 + 0(\ln^{-1/2}\Lambda_x)] \quad (18c)$$

$$\frac{C_{D,v}}{2\alpha^2} = (\gamma - 1)\frac{(Pr + 3g_w)}{3}\frac{\Lambda^2}{\ln\Lambda}[1 + 0(\ln^{-1/2}\Lambda)] \quad (18d)$$

where $C_{D,v}$ is the viscous drag coefficient referenced to base area. Equations (18a–18c) indicate that $\delta \sim x^{3/4}$, $p_e \sim x^{-1/2}$, $r_w\tau_w \sim x^0$, and $r_w q_w \sim x^0$ to within a factor $\ln\Lambda_x \sim \ln x^{3/4}/r_w$. Hence these quantities depend only weakly on the local value of $r_w$ and are otherwise independent of profile shape. Similarly, Eq. (18d) indicates that the viscous drag $D_v$ is proportional to $\bar{L}$ to within a factor $\ln\bar{L}^{3/4}/\bar{r}_w(\bar{L})$ and is also independent of upstream profile shape.

The pressure drag on an axisymmetric power-law body in the strong interaction regime is

$$C_{D,p}/2\alpha^2 = [4m/(4m - 1)](p_e)_{x=1}[1 + 0(\ln^{-1/2}\Lambda)] \quad (18e)$$

Note that $C_{D,p}/C_{D,v} \sim (\ln^{1/2}\Lambda)/\Lambda$. Thus $C_D = C_{D,v}$ to leading order.

The error in Eqs. (18) is of order $\ln^{-1/2}\Lambda_x$ so that the convergence to the limit $\Lambda_x \to \infty$ is very slow. These equations are compared in Fig. 2 for moderate values of $\Lambda_x$ with an exact solution of the local similarity equations. The comparison is discussed later. The full expression $C_D = C_{D,v} + C_{D,p}$ is used in Fig. 2e.

Equations (18) agree with the results of Ref. 6. Hence, the present local similarity method is exact in the strong interaction limit. This is due to the use of $r_e$ in Eq. (3a) (Appendix A).

### 3. *Numerical solution of local similarity equations*

Equations (14) have been solved analytically for the limiting cases of weak and strong interaction. The general case including moderate interaction requires a numerical solution. A first attempt to solve these equations by iteration starting with an assumed variation $A(x)$ did not converge. The following numerical procedure was then developed.

Let $\Phi \equiv p_e r_w r_e^\sigma A$. Differentiation of the square of Eq. (14c), so as to eliminate the integral, yields

$$\frac{d\Phi}{dx} = \frac{1}{\gamma}\left[\frac{\sigma + 1}{2}(\gamma - 1)\Lambda\right]^2\frac{r_e^\sigma}{r_w A} \quad (19a)$$

Similarly, differentiation of Eq. (14a) and neglecting a term $[\beta\partial(BJ_e)/\partial\beta]/[A\partial(BJ_e)/\partial A]$ compared with 1, yields

$$\frac{dA}{dx} = \frac{(\sigma + 1)(1 + BJ_e)}{r_e[\partial(BJ_e)/\partial A]}\left[\frac{1}{k}\left(\frac{\Phi}{r_w r_e^\sigma A}\right)^{1/2} - \frac{\dot{r}_w r_e}{r_w}\right] \quad (19b)$$

where $\partial(BJ_e)/\partial A$ is known from Eq. (11a). The explicit dependence of Eqs. (19) on $r_e$ can be removed by recalling $r_e = r_w(1 + BJ_e)^{1/(\sigma+1)}$. The strong interaction regime solution provides initial values for the integration of Eqs. (19) when $A \to \infty$ as $x \to 0$. For a specified large value of $A$, the corresponding values of $\beta$ and $x$ are given by Eqs. (17), and the value of $\Phi$ is found from

$$\Phi = A[(3kr_w)/(4x)]^2 r_w^{\sigma+1}(BJ_e)^{(\sigma+2)/(\sigma+1)}$$

¶ When $\sigma = 0$; $x^{-3/4}\delta = 2[(\gamma - 1)J_e\Lambda]^{1/2}/[3(\gamma)^{1/2}k]^{1/2} = \text{const}$. When $\sigma = 1$, $m \neq \frac{3}{4}$; $x^{-3/4}\delta \sim \ln^{-1/4}\Lambda_x$. The quantity $\ln^{-1/4}\Lambda_x$ can be treated as a constant in processes involving differentiation and integration to within an error of order $\ln^{-1}\Lambda_x$.

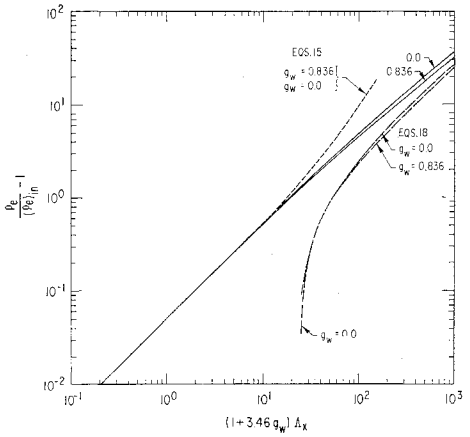


a) Surface pressure

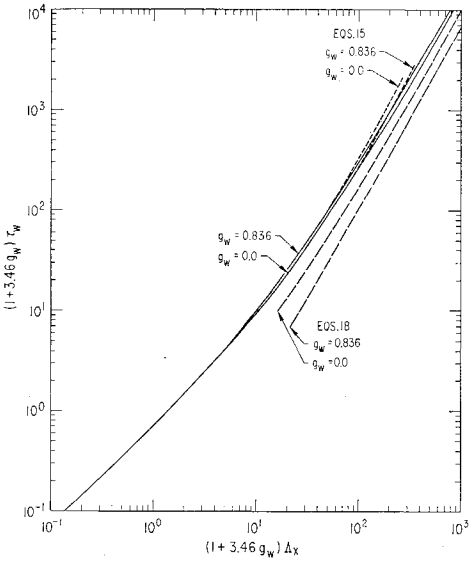


b) Local wall shear

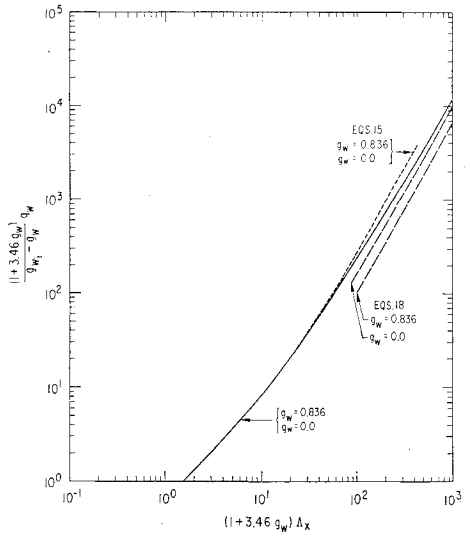


c) Local heat transfer

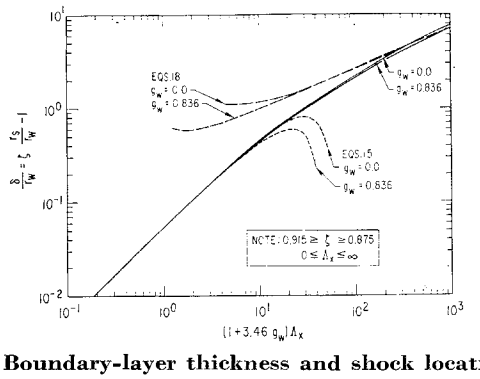


d) Boundary-layer thickness and shock location

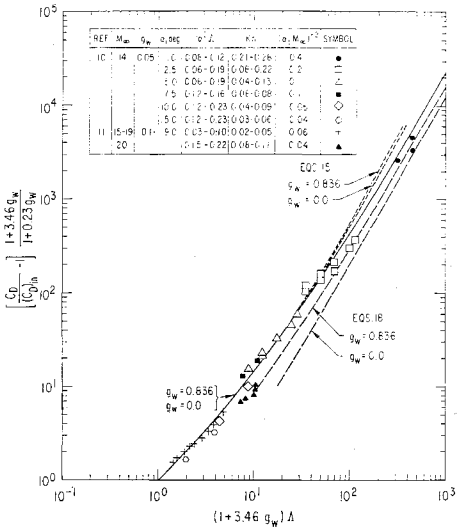


e) Drag coefficient

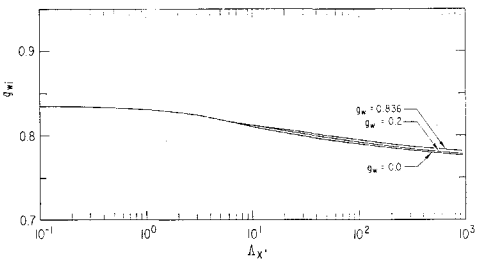


f) Recovery temperature

**Fig. 2 Local similarity solution for cone and comparison with weak interaction solution [Eq. (15)] and with strong interaction solution [Eq. (18)]; $Pr = 0.7$, $\gamma = 1.4$.**

When $A \to 0$ as $x \to 0$, the initial values are provided by conventional boundary-layer theory.

In order to integrate Eqs. (19), it is necessary to know $k$ and $\beta$ as functions of $A,x$. The evaluation of these quantities from Eqs. (7) and (14d) introduces higher order derivatives of $r_e$ and greatly complicates the solution. However, $k$ and $\beta$ do not vary greatly when going from strong-to-weak interaction (i.e., $0.91 \leq k^2 \leq 1.0$, $\frac{1}{14} \geq \beta \geq 0$ for $\gamma = 1.4$, $\sigma = 1$, $\frac{3}{4} \leq m_e \leq 1$). Hence these two variables (only) are computed by a simplified method.** It is assumed that, locally, $r_e \sim x^{m_e}$, $p_e \sim x^{2(m_e-1)}$. Thus,

$$\beta = [(\gamma - 1)/\gamma]\{2(1 - m_e)/[2m_e(\sigma + 1) - 1]\} \quad (20a)$$

** A simpler procedure is to assume that $k$ and $\beta$ are constants. This does not permit exact agreement in the limits of both weak and strong interaction.

**Table 5 Local similarity solution for cone; $Pr = 0.7$, $g_w = 0$.**

a) $\gamma = 1.4$

| $(1+3.46g_w)\Lambda_\chi$ | $\frac{p_e}{(p_e)_{in}} - 1$ | $(1+3.46g_w)\tau_w$ | $\frac{(1+3.46g_w)q_w}{g_{wi}-g_w}$ | $\left(\frac{1+3.46g_w}{1+0.23g_w}\right) \times \left(\frac{C_D}{(C_D)_{in}} - 1\right)$ | $\delta/r_w$ | $g_{wi}$ | $\frac{Kn}{\alpha(g_w)^{1/2}\Lambda_\chi}$ |
|---|---|---|---|---|---|---|---|
| 3.239E+03 | 1.092E+02 | 1.085E+05 | 1.008E+05 | 2.078E+05 | 1.358E+01 | 7.695E-01 | 1.377E-01 |
| 2.103E+03 | 7.374E+01 | 4.973E+04 | 4.597E+04 | 9.011E+04 | 1.097E+01 | 7.713E-01 | 1.434E-01 |
| 1.406E+03 | 5.121E+01 | 2.417E+04 | 2.226E+04 | 4.269E+04 | 8.975E+00 | 7.730E-01 | 1.493E-01 |
| 9.394E+02 | 3.563E+01 | 1.184E+04 | 1.086E+04 | 2.059E+04 | 7.327E+00 | 7.749E-01 | 1.559E-01 |
| 6.279E+02 | 2.483E+01 | 5.841E+03 | 5.347E+03 | 1.005E+04 | 5.965E+00 | 7.770E-01 | 1.632E-01 |
| 4.196E+02 | 1.733E+01 | 2.909E+03 | 2.657E+03 | 4.960E+03 | 4.839E+00 | 7.791E-01 | 1.714E-01 |
| 2.805E+02 | 1.211E+01 | 1.463E+03 | 1.335E+03 | 2.472E+03 | 3.908E+00 | 7.815E-01 | 1.804E-01 |
| 1.929E+02 | 8.674E+00 | 7.803E+02 | 7.115E+02 | 1.307E+03 | 3.189E+00 | 7.838E-01 | 1.895E-01 |
| 1.327E+02 | 6.208E+00 | 4.208E+02 | 3.836E+02 | 6.987E+02 | 2.587E+00 | 7.864E-01 | 1.994E-01 |
| 9.394E+01 | 4.551E+00 | 2.406E+02 | 2.193E+02 | 3.960E+02 | 2.119E+00 | 7.889E-01 | 2.091E-01 |
| 6.462E+01 | 3.239E+00 | 1.331E+02 | 1.213E+02 | 2.168E+02 | 1.692E+00 | 7.919E-01 | 2.202E-01 |
| 4.708E+01 | 2.419E+00 | 8.165E+01 | 7.439E+01 | 1.318E+02 | 1.388E+00 | 7.946E-01 | 2.299E-01 |
| 3.333E+01 | 1.749E+00 | 4.865E+01 | 4.429E+01 | 7.760E+01 | 1.107E+00 | 7.978E-01 | 2.407E-01 |
| 2.500E+01 | 1.327E+00 | 3.203E+01 | 2.913E+01 | 5.054E+01 | 9.079E-01 | 8.007E-01 | 2.497E-01 |
| 1.821E+01 | 9.721E-01 | 2.055E+01 | 1.865E+01 | 3.199E+01 | 7.221E-01 | 8.040E-01 | 2.594E-01 |
| 1.366E+01 | 7.276E-01 | 1.394E+01 | 1.262E+01 | 2.141E+01 | 5.800E-01 | 8.071E-01 | 2.678E-01 |
| 1.054E+01 | 5.577E-01 | 9.959E+00 | 8.997E+00 | 1.509E+01 | 4.717E-01 | 8.100E-01 | 2.750E-01 |
| 8.135E+00 | 4.258E-01 | 7.204E+00 | 6.491E+00 | 1.077E+01 | 3.802E-01 | 8.129E-01 | 2.815E-01 |
| 6.279E+00 | 3.245E-01 | 5.273E+00 | 4.738E+00 | 7.772E+00 | 3.038E-01 | 8.157E-01 | 2.874E-01 |
| 4.846E+00 | 2.474E-01 | 3.901E+00 | 3.495E+00 | 5.674E+00 | 2.409E-01 | 8.185E-01 | 2.926E-01 |
| 3.849E+00 | 1.947E-01 | 3.008E+00 | 2.689E+00 | 4.327E+00 | 1.950E-01 | 8.208E-01 | 2.965E-01 |
| 2.971E+00 | 1.490E-01 | 2.261E+00 | 2.016E+00 | 3.219E+00 | 1.529E-01 | 8.232E-01 | 3.002E-01 |
| 2.360E+00 | 1.177E-01 | 1.763E+00 | 1.569E+00 | 2.491E+00 | 1.228E-01 | 8.251E-01 | 3.030E-01 |
| 1.874E+00 | 9.314E-02 | 1.380E+00 | 1.226E+00 | 1.937E+00 | 9.843E-02 | 8.268E-01 | 3.053E-01 |
| 1.489E+00 | 7.377E-02 | 1.083E+00 | 9.613E-01 | 1.513E+00 | 7.873E-02 | 8.283E-01 | 3.072E-01 |
| 1.183E+00 | 5.847E-02 | 8.527E-01 | 7.556E-01 | 1.186E+00 | 6.287E-02 | 8.296E-01 | 3.088E-01 |
| 9.128E-01 | 4.504E-02 | 6.527E-01 | 5.778E-01 | 9.048E-01 | 4.875E-02 | 8.308E-01 | 3.102E-01 |
| 7.250E-01 | 3.573E-02 | 5.155E-01 | 4.560E-01 | 7.129E-01 | 3.885E-02 | 8.317E-01 | 3.112E-01 |
| 5.759E-01 | 2.836E-02 | 4.077E-01 | 3.603E-01 | 5.626E-01 | 3.094E-02 | 8.325E-01 | 3.120E-01 |
| 4.575E-01 | 2.251E-02 | 3.227E-01 | 2.850E-01 | 4.446E-01 | 2.463E-02 | 8.331E-01 | 3.127E-01 |
| 3.634E-01 | 1.788E-02 | 2.556E-01 | 2.257E-01 | 3.518E-01 | 1.959E-02 | 8.336E-01 | 3.132E-01 |
| 2.886E-01 | 1.421E-02 | 2.026E-01 | 1.788E-01 | 2.785E-01 | 1.558E-02 | 8.340E-01 | 3.137E-01 |

b) $\gamma = 5/3$

| $(1+3.46g_w)\Lambda_\chi$ | $\frac{p_e}{(p_e)_{in}} - 1$ | $(1+3.46g_w)\tau_w$ | $\frac{(1+3.46g_w)q_w}{g_{wi}-g_w}$ | $\left(\frac{1+3.46g_w}{1+0.33g_w}\right) \times \left(\frac{C_D}{(C_D)_{in}} - 1\right)$ | $\delta/r_w$ | $g_{wi}$ | $\frac{Kn}{\alpha(g_w)^{1/2}\Lambda_\chi}$ |
|---|---|---|---|---|---|---|---|
| 2.127E+03 | 1.073E+02 | 7.913E+04 | 7.283E+04 | 1.479E+05 | 1.336E+01 | 7.677E-01 | 1.797E-01 |
| 1.381E+03 | 7.244E+01 | 3.626E+04 | 3.323E+04 | 6.415E+04 | 1.080E+01 | 7.695E-01 | 1.871E-01 |
| 9.233E+02 | 5.031E+01 | 1.763E+04 | 1.609E+04 | 3.040E+04 | 8.831E+00 | 7.713E-01 | 1.947E-01 |
| 6.171E+02 | 3.500E+01 | 8.630E+03 | 7.852E+03 | 1.466E+04 | 7.208E+00 | 7.732E-01 | 2.033E-01 |
| 4.124E+02 | 2.440E+01 | 4.259E+03 | 3.865E+03 | 7.162E+03 | 5.867E+00 | 7.752E-01 | 2.128E-01 |
| 2.756E+02 | 1.703E+01 | 2.121E+03 | 1.921E+03 | 3.535E+03 | 4.758E+00 | 7.774E-01 | 2.233E-01 |
| 1.896E+02 | 1.221E+01 | 1.120E+03 | 1.013E+03 | 1.852E+03 | 3.902E+00 | 7.796E-01 | 2.340E-01 |
| 1.267E+02 | 8.526E+00 | 5.687E+02 | 5.144E+02 | 9.329E+02 | 3.135E+00 | 7.822E-01 | 2.466E-01 |
| 8.716E+01 | 6.104E+00 | 3.066E+02 | 2.774E+02 | 4.991E+02 | 2.542E+00 | 7.849E-01 | 2.592E-01 |
| 6.171E+01 | 4.476E+00 | 1.753E+02 | 1.586E+02 | 2.832E+02 | 2.082E+00 | 7.875E-01 | 2.714E-01 |
| 4.368E+01 | 3.273E+00 | 1.014E+02 | 9.180E+01 | 1.625E+02 | 1.693E+00 | 7.904E-01 | 2.843E-01 |
| 3.093E+01 | 2.383E+00 | 5.947E+01 | 5.385E+01 | 9.451E+01 | 1.364E+00 | 7.935E-01 | 2.975E-01 |
| 2.253E+01 | 1.772E+00 | 3.697E+01 | 3.347E+01 | 5.824E+01 | 1.109E+00 | 7.965E-01 | 3.098E-01 |
| 1.642E+01 | 1.309E+00 | 2.332E+01 | 2.111E+01 | 3.639E+01 | 8.929E-01 | 7.998E-01 | 3.219E-01 |
| 1.231E+01 | 9.882E-01 | 1.556E+01 | 1.407E+01 | 2.404E+01 | 7.258E-01 | 8.029E-01 | 3.327E-01 |
| 9.233E+00 | 7.412E-01 | 1.054E+01 | 9.512E+00 | 1.609E+01 | 5.839E-01 | 8.062E-01 | 3.431E-01 |
| 6.923E+00 | 5.526E-01 | 7.246E+00 | 6.526E+00 | 1.093E+01 | 4.647E-01 | 8.095E-01 | 3.528E-01 |
| 5.343E+00 | 4.227E-01 | 5.240E+00 | 4.709E+00 | 7.805E+00 | 3.747E-01 | 8.125E-01 | 3.607E-01 |
| 4.124E+00 | 3.226E-01 | 3.834E+00 | 3.438E+00 | 5.640E+00 | 2.997E-01 | 8.154E-01 | 3.679E-01 |
| 3.183E+00 | 2.463E-01 | 2.836E+00 | 2.537E+00 | 4.121E+00 | 2.378E-01 | 8.183E-01 | 3.741E-01 |
| 2.528E+00 | 1.940E-01 | 2.186E+00 | 1.951E+00 | 3.145E+00 | 1.926E-01 | 8.206E-01 | 3.789E-01 |
| 2.008E+00 | 1.531E-01 | 1.695E+00 | 1.510E+00 | 2.417E+00 | 1.553E-01 | 8.228E-01 | 3.830E-01 |
| 1.550E+00 | 1.175E-01 | 1.280E+00 | 1.139E+00 | 1.811E+00 | 1.215E-01 | 8.250E-01 | 3.869E-01 |
| 1.231E+00 | 9.300E-02 | 1.002E+00 | 8.897E-01 | 1.409E+00 | 9.738E-02 | 8.267E-01 | 3.897E-01 |
| 9.780E-01 | 7.368E-02 | 7.866E-01 | 6.975E-01 | 1.101E+00 | 7.791E-02 | 8.282E-01 | 3.920E-01 |
| 7.768E-01 | 5.841E-02 | 6.190E-01 | 5.483E-01 | 8.631E-01 | 6.224E-02 | 8.295E-01 | 3.940E-01 |
| 6.171E-01 | 4.632E-02 | 4.880E-01 | 4.319E-01 | 6.784E-01 | 4.966E-02 | 8.306E-01 | 3.956E-01 |
| 4.901E-01 | 3.676E-02 | 3.853E-01 | 3.407E-01 | 5.344E-01 | 3.959E-02 | 8.316E-01 | 3.969E-01 |
| 3.893E-01 | 2.917E-02 | 3.046E-01 | 2.692E-01 | 4.217E-01 | 3.153E-02 | 8.324E-01 | 3.979E-01 |
| 3.093E-01 | 2.316E-02 | 2.411E-01 | 2.129E-01 | 3.333E-01 | 2.510E-02 | 8.330E-01 | 3.987E-01 |
| 2.457E-01 | 1.839E-02 | 1.909E-01 | 1.686E-01 | 2.636E-01 | 1.998E-02 | 8.335E-01 | 3.994E-01 |
| 1.951E-01 | 1.461E-02 | 1.513E-01 | 1.335E-01 | 2.087E-01 | 1.589E-02 | 8.340E-01 | 4.000E-01 |

$$k^2 = k_1^2\left[1 + \frac{k_2}{\sigma+1}\frac{m_e-1}{m_e} + k_3\left(\frac{m_e-1}{(\sigma+1)m_e}\right)^2 + \cdots\right] \tag{20b}$$

where

$$m_e = \frac{(1+\phi)^2}{1 - (\ddot{r}_w r_w/\dot{r}_w^2) - \phi[(\ddot{B}/\dot{B})(r_w/\dot{r}_w) - (\sigma+1)\phi]} \tag{20c}$$

$$\phi \equiv \frac{r_w\dot{r}_e}{\dot{r}_w r_e} - 1 = \frac{1}{\sigma+1}\frac{r_w}{\dot{r}_w}\frac{\dot{B}}{B}\frac{BJ_e}{1+BJ_e} \tag{20d}$$

Equation (20c) is obtained from Eqs. (7c) and (14a), assuming that derivatives of $J_e$ with respect to $x$ can be neglected (since $J_e$ is a slowly varying function of $\beta$ and $A$). For power-law bodies, $B \sim x^N$ and

$$\frac{\ddot{B}}{\dot{B}}\frac{r_w}{\dot{r}_w} = \frac{N-1}{m} \qquad \frac{r_w}{\dot{r}_w}\frac{\dot{B}}{B} = \frac{N}{m} \tag{21a}$$

where

$$N = (\sigma-1)m_e + (\tfrac{3}{2}) - (\sigma+1)m \tag{21b}$$

In the case of power-law bodies, Eqs. (20) and (21) are functions only of $A$ and are solved by iteration. The resulting solution for $k$ and $\beta$ is exact in the limits of strong and weak interaction and is probably accurate to within a few percent in the intermediate region. Equations (19) can then be integrated to find $\Phi$ and $A$ as functions of $x$. After evaluation of the integral in Eqs. (8), all local boundary-layer properties can be readily found.

The local similarity equations have been integrated numerically (starting at $A = 750$) for hypersonic flow over a cone. It was assumed that $\gamma = \frac{7}{5}, \frac{5}{3}$; $P_r = 0.7$; and $g_w = 0$, 0.2, and 0.836. Major results (for the range $A \lesssim 100$) are shown in Table 5 and Fig. 2. The effect of $g_w$ on $p_e$, $\delta$, $\tau_w$, $q_w$, and $C_D$ has been correlated to within about 10% for $\Lambda_x \lesssim 10^3$ by expressing these variables as noted in Table 5 and Fig. 2. The correlations are motivated by (and are exact for) the weak interaction limit and are approximately correct for the strong interaction regime.

The weak interaction solution, Eqs. (15), and the strong interaction solution, Eqs. (18), are included in Fig. 2. The weak interaction solution agrees with the numerical local similarity solution to within a few percent for $\Lambda_x \lesssim 10$; the results for shear, heat transfer, and drag agree to within about 20% for $\Lambda_x \lesssim 100$. The strong interaction solution agrees with the numerical local similarity solution to within ~50% at $\Lambda_x = 100$ and converges very slowly to this solution with increase in $\Lambda_x$.

Experimental results for cone drag obtained from Refs. 10 and 11 are included in Fig. 2e. Corresponding values of $\alpha^2\Lambda$, $K_n$, and $(\alpha_s M_\infty)^{-2}$ are also noted. As later discussed in Appendix B, $\alpha^2\Lambda$ is a measure of shock-layer rarefaction effects, and $K_n$ is a measure of wall slip. Both should be small for the present theory to apply. The quantity $(\alpha_s M_\infty)^{-2}$ is a measure of shock strength and has also been assumed small. The experimental data for $M_\infty = 15$ to 19 and a 9° cone comes closest to meeting the requirements of small $\alpha^2\Lambda$, $K_n$, and $(\alpha_s M_\infty)^{-2}$ and is in very good agreement with the theory. However, these data represent a relatively weak interaction. The remaining data are scattered about the theoretical curve. There is good "average" agreement. In the strong interaction regime, the experimental data for a given cone angle generally exhibits a lower slope $dC_D/d\Lambda$ than indicated by the present theory. This may be due to the increase of rarefaction effects [i.e., the spread in the values of $\alpha^2\Lambda$ and $K_n$, indicated in Fig. 2e, are associated with the lowest and highest values of $\Lambda$ for each cone angle].

The local values of $\bar{p}_e$, $\bar{r}_e$, $\bar{\tau}_w$, and $\bar{q}_w$ in the strong interaction regime are independent of upstream body profile shape and depend only on the local values of $\bar{r}_w, \bar{x}$ [Eqs. (18)]. Hence Fig. 2 and Table 5 can be used to estimate flow properties on arbitrary slender axisymmetric bodies, in the strong interaction regime, provided $\alpha$ and $\bar{L}$ are replaced by $\bar{r}_w/\bar{x}$ and $\bar{x}$.

## III. Concluding Remarks

Viscous interaction has been considered for the case of hypersonic flow over slender bodies. It has been assumed that the shock slope is small, that the shock is strong, and that local surface pressure depends only on local effective body shape [Eq. (7)]. Both two-dimensional and axisymmetric bodies have been treated in a unified manner. However, only the axisymmetric case has been considered in detail. The independent variable $\xi$, Eq. (3a), has been based on $r_e$ rather than $r_w$ as the characteristic boundary-layer ordinate. This formulation was necessary in order that the local similarity solution for axisymmetric bodies agree with the exact solution, in the limit of strong interaction.

The nondimensional equations of motion and boundary conditions indicate that for geometrically similar bodies [same $r_w(x)$], the parameters that define the flowfield are $\gamma$, $Pr$, $g_w$, $F_w$, and an interaction parameter $\Lambda$. Numerical results have been obtained for cones that cover the entire spectrum for strong to weak interaction. Effects of wall temperature were correlated to within ~10% by expressing the dependent and independent variables in a form suggested by the weak interaction solution.

The assumed dependence of $p_e$ on $r_e$, Eqs. (7), is exact in the limit of no interaction over power-law bodies and for strong interaction over arbitrary bodies. The local similarity equations, Eqs. (14), are also exact in these limits. Hence the present solution should be reasonably accurate in the intermediate regime. Dewey[12] assumed a tangent wedge pressure relation and obtained an approximate local similarity solution for the two-dimensional viscous interaction problem. His solution also was exact in the limits of weak and strong interaction. Comparison with more accurate two-dimensional solutions indicated an accuracy of ~10 to 15% in the intermediate regime. A similar accuracy is expected herein.

## Appendix A: Comparison with Reference 7

The definition of $\xi$ [Eq. (3a)] contains $r_e$ rather than $r_w$ as the characteristic boundary-layer ordinate. This choice is necessary in order that the local similarity solution be in agreement with the exact solution in the limit of strong interaction over axisymmetric bodies.†† Since Ref. 7 is based on $r_w$ (as are Refs. 4 and 6), the relationship between the two approaches is of interest.

Define new variables as follows (denoted by superscript ~):

$$\tilde{\xi} \equiv \left(\int_0^x p_e r_w^{2\sigma}dx\Big/\int_0^x p_e r_e^{2\sigma}dx\right)\xi = \int_0^\xi\left(\frac{r_w}{r_e}\right)^{2\sigma}d\xi$$

$$\tilde{\eta} = \left(\frac{\xi}{\tilde{\xi}}\right)^{1/2}\eta$$

$$\tilde{F}(\tilde{\xi},\tilde{\eta}) = (\xi/\tilde{\xi})^{1/2}F(\xi,\eta) \qquad \tilde{G}(\tilde{\xi},\tilde{\eta}) = G(\xi,\eta)$$

$$\tilde{R}(\tilde{\xi},\tilde{\eta})\ 1 + A\int_0^{\tilde{\eta}}[\tilde{G} - (F_{\tilde{\eta}})^2]d\tilde{\eta} = \left(\frac{r}{r_w}\right)^{\sigma+1}$$

$$\tilde{R}(\tilde{\xi},\infty) \equiv 1 + AI_e = 1 + BJ_e$$

†† It was stated in Ref. 7 that the formulation therein did agree with the exact solution in the limit of strong interaction on axisymmetric bodies. This was due to the assumed form of Eq. (28b) in Ref. 7. However, within the framework of a local similarity solution, the quantity $m$ in Eq. (28b) should be replaced by $\frac{3}{4}$. This will lead to small errors in pressure and displacement thickness for bodies, other than a $\frac{3}{4}$ power law, in the strong interaction limit. In particular, $p_e$ and $\delta$ will be in error due to factors $[m + (\frac{1}{4})]^{-1/2}$ and $[m + (\frac{1}{4})]^{-1/4}$, respectively.

The superscripted variables represent the conventional boundary-layer formulation. (These variables appear without the superscripts in Ref. 7.) It then follows that $AI_e = BJ_e$, $A = B(\bar{\xi}/\xi)^{1/2}$. For self-similar flows, $r_w/r_e$ is constant and $\bar{\xi}/\xi = (r_w/r_e)^{2\sigma}$. In terms of the new variables, the momentum and energy equations have the same form as Eqs. (5a) and (5b) except that the factor $(r_w/r_e)^{2\sigma}$ does not appear. The solution of these equations is therefore simplified. Numerical solutions for the case of self-similar flow are given in Ref. 7. These are correlated in Ref. 7 by analytic expressions. The correlations are used herein, which explains the appearance of $A$ in the present study.

The local similarity equations were simplified in Ref. 7 to a series of algebraic equations. These represented a generalization of Dewey's method[12] to $\sigma = 1$. The simplified equations were evaluated and results tabulated for flow over a cone in the range $\Lambda_x \lesssim 10^3$. The numerical cone results presented here agree with those in Ref. 7 to within 10 to 15%, which is within the expected accuracy of the local similarity equations. Hence, the present use of $r_e$ is motivated primarily by the esthetic desire for exact agreement in the limit of strong interaction rather than for significant improvement in numerical accuracy. Also, the present integration of the full local similarity equation, rather than a simplified version of these equations (as in Ref. 7), eliminates errors and uncertainty from this source.

## Appendix B: Rarefaction Effects

Criteria that define the onset of rarefaction effects in the shock layer and at the body surface are noted. With increase in the "rarefaction parameter," $M_\infty(C/Re)^{1/2} \equiv \alpha^2\Lambda$ the boundary layer and shock wave thicken and finally merge. This merging has not been considered in the present model that assumes an isentropic, irrotational local freestream external to the boundary layer. S. M. Bogdonoff has observed (in a private communication) that merging occurs at $\alpha^2\Lambda \doteq 0.2$ for cones. Merging reduces surface pressure[13] and thereby tends to reduce surface shear, heat transfer, and drag.

At the body surface, rarefaction results in velocity slip and temperature jump. A suitable parameter defining this effect is

$$Kn \equiv \bar{\lambda}_w(\partial\bar{u}/\partial\bar{r})_w/\bar{u}_e \doteq \bar{u}_w/\bar{u}_e \tag{B1}$$

where $Kn$ is a Knudsen number, $\bar{u}_w$ is the velocity (slip) at the wall, and $\bar{\lambda}_w$ is the mean free path at the wall. In nondimensional variables, assuming $\bar{\lambda} = (\pi\gamma/2)^{1/2}(\bar{\mu}/\bar{\rho}\bar{a})$, $M_\infty^2 \gg 1$, where $\bar{a}$ is the speed of sound

$$\frac{Kn}{\alpha\Lambda(g_w)^{1/2}} = \frac{1}{2}\left(\frac{(\gamma-1)\pi}{\gamma}\right)^{1/2}\frac{\tau_w}{\Lambda p_e} \tag{B2}$$

For cones, $Kn/[\alpha(g_w)^{1/2}\Lambda_x]$ equals 0.32 at $\Lambda_x = 0$ ($\gamma = 1.4$), and decreases slowly with increase in $\Lambda_x$. Numerical results are given in Tables 2 and 5. Surface slip also tends to reduce the magnitude of the surface pressure, shear, etc. and should be considered for values of $Kn$ greater than ~0.1 or 0.2.

## References


[1] Hayes, W. D. and Probstein, R. F., *Hypersonic Flow Theory*, Academic, New York, 1959, pp. 333–370.

[2] Probstein, R. F. and Elliott, D., "The Transverse Curvature Effect in Compressible Axially Symmetric Laminar Boundary Layer Flow," *Journal of Aeronautical Sciences*, Vol. 23, No. 3, 1956, p. 258.

[3] Probstein, R. F., "Interacting Hypersonic Laminar Boundary Layer Flow over a Cone," AF 2798/1, Brown Univ., Div. of Engineering, Providence, R. I.; also Contract AF 33(616)-2798, March 1955.

[4] Yasuhara, M., "Axisymmetric Viscous Flow past Very Slender Bodies of Revolution," *Journal of the Aerospace Sciences*, Vol. 29, No. 6, 1962, p. 667.

[5] Stewartson, K., "Viscous Hypersonic Flow past a Slender Cone," *The Physics of Fluids*, Vol. 7, No. 5, 1964, p. 667.

[6] Ellinwood, J. W. and Mirels, H., "Axisymmetric Hypersonic Flow with Strong Viscous Interaction," TR-1001(2240-10)-11, July 1967, Aerospace Corp.; also *Journal of Fluid Mechanics* (to be published).

[7] Mirels, H. and Ellinwood, J. W., "Hypersonic Viscous Interaction Theory for Slender Axisymmetric Bodies," Paper 68-1, Jan. 1968, AIAA.

[8] Mirels, H., "Hypersonic Flow over Slender Bodies Associated with Power Law Shocks," *Advances in Applied Mechanics*, Vol. 7, Academic, New York, 1962.

[9] Cheng, H. K. et al., "Boundary Layer Displacement and Leading Edge Bluntness effects in High Temperature Hypersonic Flow," *Journal of the Aerospace Sciences*, Vol. 28, No. 5, 1961, p. 353.

[10] Kussoy, M., "Hypersonic Viscous Drag on Cones in Rarefied Flow," TN D-4036, June 1967, NASA.

[11] Whitfield, J. D. and Griffith, B. J., "Viscous Drag Effects on Slender Cones in Low Density Hypersonic Flow," *AIAA Journal*, Vol. 3, No. 6, June 1965, p. 1165.

[12] Dewey, C. F., Jr., "Use of Local Similarity Concepts in Hypersonic Viscous Interaction Problems," *AIAA Journal*, Vol. 1, No. 1, Jan. 1963, p. 20.

[13] McCroskey, W. J., Bogdonoff, S. M., and Genchi, A. P., "Leading Edge Flow Studies of Sharp Bodies in Rarefied Hypersonic Flow," *Proceedings of the 5th International Symposium on Rarefied Gas Dynamics, II*, Academic, New York, 1967.